

LIBRARY
ROYAL AIRCRAFT ESTABLISHMENT
BEDFORD.

R. & M. No. 2923
(15,670, 16,130)
A.R.C. Technical Report



MINISTRY OF SUPPLY

AERONAUTICAL RESEARCH COUNCIL
REPORTS AND MEMORANDA

Hinge-moment Derivatives for an Oscillating Control

By

C. S. SINNOTT
of the Aerodynamics Division, N.P.L.

Crown Copyright Reserved

LONDON: HER MAJESTY'S STATIONERY OFFICE

1955

PRICE 3s 6d NET

Hinge-moment Derivatives for an Oscillating Control

By

C. S. SINNOTT

of the Aerodynamics Division, N.P.L.

*Reports and Memoranda No. 2923**

September, 1953

Summary.—The semi-empirical 'equivalent profile' method of W. P. Jones¹ (1948) is extended to the case of an aerofoil with an oscillating control. The oscillatory hinge-moment derivatives for such an aerofoil-control combination in a low-speed wind tunnel are estimated, an allowance for tunnel wall interference effects being included.

A comparison with measured values of the control derivatives is made for two values of the control chord ratio, representing an aileron and a tab. The method of this report gives results in much better agreement with experiment than those obtained by vortex-sheet theory².

1. *Introduction.*—The oscillatory hinge-moment derivatives for a 15 per cent thick aerofoil (NPL 282) with a 20 per cent trailing-edge control have been measured by Wight³ (1952). These results show substantially the same variation with frequency parameter as those estimated by vortex-sheet theory, but they are reduced in magnitude by a factor that is approximately constant. This reduction factor varies with Reynolds number and transition position over the range 0.5 to 0.7 for h_p , and 0.55 to 0.65 for $h_{\dot{p}}$. The discrepancy between the measured values of the derivatives and those estimated by vortex-sheet theory is thought to be due in part to the effects of thickness and viscosity.

In this report some account of thickness/chord ratio and boundary-layer effects is taken by the replacement of the thick aerofoil by a thin 'equivalent' profile. This equivalent profile is chosen to give approximately the same measured lift distribution in steady motion as that for the original aerofoil-control combination at a particular control incidence, and for a particular Reynolds number and transition position. It is assumed that the equivalent profile deforms in phase with the control oscillation and the aerodynamic forces are then calculated by linearized theory.

From the above assumption it might be expected that there would be a considerable discrepancy between estimated and measured values of the derivatives for high values of the frequency parameter. This was not found to be so for the aerofoil-control combinations considered for a range of frequency parameter extending up to $\omega = 2.0$, as is shown in Figs. 4, 5, 6 and 7.

* Published with the permission of the Director, National Physical Laboratory.

2. *Theory.*—(a) *Steady Flow.*—It is assumed that the flow about a thick aerofoil-control combination can be reproduced approximately by a thin profile which has the same lift distribution in steady motion.

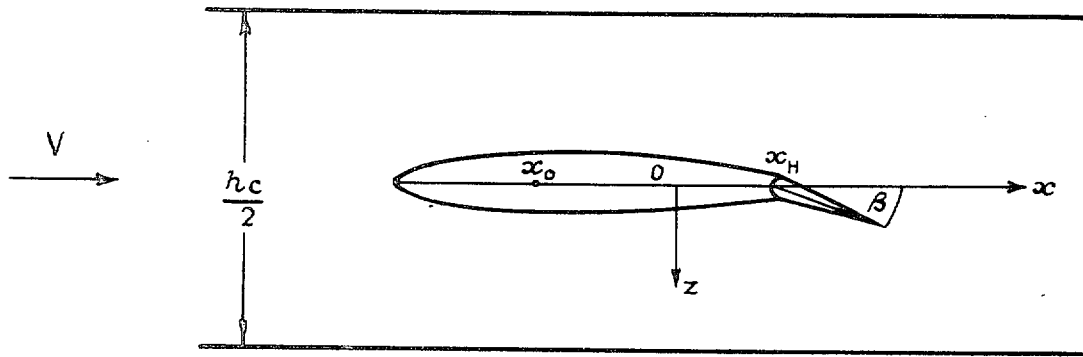


FIG. 1.

Let the origin of co-ordinates (x, z) be taken at the mid-chord point, and put $x = -\frac{1}{2}c \cos \theta$.

Then suppose the lift-distribution over the aerofoil-control combination in steady motion can be represented by

$$l(\theta) = \rho V^2 (A_0 \bar{F}_0 + A_1 \bar{F}_1 + A_2 \bar{F}_2 + \dots) \quad \dots \quad \dots \quad \dots \quad (1)$$

where the A_n 's are functions of β only and \bar{F}_n is defined in the list of symbols.

The corresponding steady-motion coefficients of lift, pitching moment, and hinge moment are then given by

$$\left. \begin{aligned} C_L &= \int_0^\pi L(\theta) \sin \theta \, d\theta \\ C_M(x_0) &= \frac{1}{2} \int_0^\pi L(\theta) (\cos \theta - \cos \theta_0) \sin \theta \, d\theta \\ C_H &= \frac{1}{2} \int_{\theta_H}^\pi L(\theta) (\cos \theta - \cos \theta_H) \sin \theta \, d\theta \end{aligned} \right\} \dots \dots \dots (2)$$

where $L(\theta) = l(\theta)/\rho V^2$.

If it is assumed that $A_n = 0$, $n \geq 3$, then the first three coefficients of (1) can be determined from experimentally obtained free-stream values of C_L , C_M , and C_H for a given aerofoil-control combination. In general it is more convenient to evaluate $dA_n/d\beta$, $n = 0, 1, 2$, from experimental values of the derivatives a_2 , m_2 , and b_2 , defined in the list of symbols. Differentiation of equations (2), with $dA_n/d\beta = A_n'$, gives

$$\left. \begin{aligned} a_2 &= 2\pi A_0' \\ m_2(x_0) &= \pi \left\{ A_0' \left(\frac{1}{2} + x_0 \right) + \frac{A_1' - A_2'}{4} \right\} \\ b_2 &= \frac{1}{E^2} \left\{ A_0' I_1 + A_1' \left(\frac{I_1}{2} - I_2 \right) - A_2' I_3 \right\} \end{aligned} \right\} \dots \dots \dots (3)$$

where the I_n 's are given in the Appendix.

The lift distribution $l(\theta)$ corresponds to a downwash distribution,

$$\frac{W}{V} = \frac{\partial z}{\partial x} = A_0 + A_1\left(\frac{1}{2} + \cos \theta\right) + A_2 \cos 2\theta + \dots \quad \dots \quad \dots \quad (4)$$

where according to linearized theory z defines the shape of the equivalent thin profile.

On integration (4) gives

$$\frac{2z}{c} = A_0 + A_1 - \frac{A_2}{3} + \left(A_0 + \frac{A_1}{2} - A_2\right)\xi - \frac{A_1}{2}\xi^2 + \frac{2}{3}A_2\xi^3 \quad \dots \quad \dots \quad (5)$$

where $\xi = -\cos \theta$ (i.e., $x = \frac{1}{2}c\xi$), and the first three terms only of (4) have been taken. The constant of integration is determined by the assumption that the leading edges of the original and equivalent profiles coincide.

(b) *Unsteady Flow.*—Let the control oscillate about $\eta = 0$, then in the complex notation for simple harmonic oscillations, the control angle $\beta = \beta_0 e^{i\omega t}$.

If $W(t)$ is the downwash due to the oscillation of the profile defined by (5), then

$$\begin{aligned} W(t) &= \frac{\partial z}{\partial t} + V \frac{\partial z}{\partial x} \\ &= \frac{\partial z}{\partial \beta} \dot{\beta} + V \frac{\partial z}{\partial x} \quad \dots \quad (6) \end{aligned}$$

where $\dot{\beta} = \partial \beta / \partial t$. When β is small, A_n is assumed to be a linear function of β , so that $A_n(\beta) = \beta A_n'(0)$. Hence, from (5) and (6),

$$\begin{aligned} W(t) &= \dot{\beta} \frac{c}{2} \left\{ A_0'(0) + A_1'(0) - \frac{A_2'(0)}{3} + \left(A_0'(0) + \frac{A_1'(0)}{2} - A_2'(0) \right) \xi - \frac{A_1'(0)}{2} \xi^2 + \frac{2}{3} A_2'(0) \xi^3 \right\} \\ &\quad + V \dot{\beta} \left\{ A_0'(0) + \frac{A_1'(0)}{2} - A_2'(0) - A_1'(0)\xi + 2A_2'(0)\xi^2 \right\}, \end{aligned}$$

which may be written

$$W(t) = V \{ C_0 + C_1\left(\frac{1}{2} + \cos \theta\right) + C_2 \cos 2\theta + C_3 \cos 3\theta \}, \quad \dots \quad \dots \quad \dots \quad (7)$$

where

$$\left. \begin{aligned} C_0 &= \dot{\beta} \left\{ A_0'(0) + i\bar{\omega} \left(\frac{3}{2} A_0'(0) + A_1'(0) - \frac{7}{12} A_2'(0) \right) \right\} \\ C_1 &= \dot{\beta} \left\{ A_1'(0) - i\bar{\omega} \left(A_0'(0) + \frac{A_1'(0) - A_2'(0)}{2} \right) \right\} \\ C_2 &= \dot{\beta} \left\{ A_2'(0) - i\bar{\omega} \frac{A_1'(0)}{4} \right\} \\ C_3 &= -\dot{\beta} i\bar{\omega} \frac{A_2'(0)}{6} \end{aligned} \right\} \quad \dots \quad \dots \quad \dots \quad (8)$$

The lift distribution $l(\theta, \bar{\omega})$ corresponding to the downwash given by (7) is readily obtained from well-known results in vortex-sheet theory⁴. It may be shown to be

$$l(\theta, \bar{\omega}) = \rho V^2 \{ C_0 \Gamma_0 + C_1 \Gamma_1 + C_2 \Gamma_2 + C_3 \Gamma_3 \} \quad \dots \quad \dots \quad \dots \quad \dots \quad \dots \quad (9)$$

where Γ_n is given in the list of symbols.

The hinge moment due to the oscillation is then given by

$$\begin{aligned} \frac{H}{\rho V^2 c^2} &= \beta \{h_\beta + i\omega h_\beta - \omega^2 h_\beta\} \\ &= \frac{1}{4} \int_{\theta_H}^{\pi} L(\theta, \bar{\omega}) (\cos \theta - \cos \theta_H) \sin \theta d\theta \\ &= \frac{1}{4} \{C_0 M_0 + C_1 M_1 + C_2 M_2 + C_3 M_3\} \end{aligned}$$

where

$$\begin{aligned} M_0 &= \int_{\theta_H}^{\pi} \Gamma_0 (\cos \theta - \cos \theta_H) \sin \theta d\theta = 2C(\bar{\omega}) I_1 + 2i\bar{\omega} I_2 \\ M_1 &= \int_{\theta_H}^{\pi} \Gamma_1 (\cos \theta - \cos \theta_H) \sin \theta d\theta = I_1 - 2I_2 + i\bar{\omega} \left(I_2 + \frac{I_3}{2} \right) \\ M_2 &= \int_{\theta_H}^{\pi} \Gamma_2 (\cos \theta - \cos \theta_H) \sin \theta d\theta = -2I_3 + i\bar{\omega} \left(\frac{I_4}{3} - I_2 \right) \\ M_3 &= \int_{\theta_H}^{\pi} L_3 (\cos \theta - \cos \theta_H) \sin \theta d\theta = -2I_4 + i\bar{\omega} \left(\frac{I_5}{4} - \frac{I_3}{2} \right). \end{aligned}$$

3. *Interference Effects.*—In the case of an aerofoil oscillating in a wind tunnel, the lift distribution (9), must be modified to allow for the presence of the tunnel walls.

Let the oscillatory lift distribution for this system be

$$l'(\theta, \bar{\omega}) = \rho V^2 \{C_0' \Gamma_0 + C_1' \Gamma_1 + C_2' \Gamma_2 + C_3' \Gamma_3\} \dots \dots \dots \dots \quad (10)$$

Then the downwash distribution corresponding to the vorticity distribution on the actual aerofoil and its wake is

$$\frac{W_T(t)}{V} = C_0' + C_1' \left(\frac{1}{2} + \cos \theta \right) + C_2' \cos 2\theta + C_3' \cos 3\theta \dots \dots \dots \dots \quad (11)$$

Furthermore it is shown in Ref. 5 that the downwash distribution over the aerofoil, induced by the infinite system of image vorticity distributions, is

$$\frac{W_I(t)}{V} = a_0 + a_1 \cos \theta + a_2 \cos 2\theta + a_3 \cos 3\theta + \dots \dots \dots \dots \quad (12)$$

$$\text{where } \left. \begin{aligned} a_0 &= -\frac{\pi^2}{6h^2} \left\{ C_0' \left(\frac{1}{2} - \frac{iC(\bar{\omega})}{\bar{\omega}} \right) + \frac{C_1' - C_2'}{4} \right\} + C_0' F J_0(\bar{\omega}) \\ a_n &= 2i^n J_n(\bar{\omega}) F C_0', \dots \dots \dots n \geq 1 \end{aligned} \right\} \dots \quad (13)$$

and F and $J_n(\bar{\omega})$ are defined in the list of symbols.

The total downwash distribution over the aerofoil-control combination is that due to the vorticity distribution over the aerofoil and its wake plus that induced by the image vorticity distributions. This must be equal to the prescribed distribution given by (7). Hence from (7), (11), and (12),

$$W(t) = W_T(t) + W_I(t)$$

and a comparison of coefficients yields

$$\left. \begin{aligned} C_0 + \frac{C_1}{2} &= C_0' + \frac{C_1'}{2} + a_0 \\ C_n &= C_n' + a_n \dots \dots n = 1, 2, 3 \end{aligned} \right\} \dots \dots \dots \dots \dots \dots (14)$$

where C_0, C_1, C_2 and C_3 are defined by (8). It then follows from (13) and (14) that

$$\begin{aligned} C_0' &= \beta R/D, \\ C_n' &= C_n - 2i^n J_n(\bar{\omega}) F C_0' \dots \dots n \geq 1, \end{aligned}$$

where R is a function of $\left. \frac{dA_n}{d\beta} \right|_{\beta=0}$, $n = 1, 2, 3$, and $\bar{\omega}$.

$$D = 1 - \frac{\pi^2}{6h^2} \left(\frac{C(\bar{\omega})}{i\bar{\omega}} + \frac{1}{2} \right) + F \left\{ J_0 - iJ_1 + \frac{\pi^2}{12h^2} (J_2 + iJ_1) \right\}.$$

The corresponding lift distribution is given by (10), and the hinge-moment derivatives may then be estimated as in section 2(b).

As $\bar{\omega} \rightarrow 0$

$$D \rightarrow \left(1 - \frac{\pi^2}{6h^2} \right) C(\bar{\omega}) + i\bar{\omega} \bar{E}, \quad \bar{E} = \log_e \frac{2 \left(1 + \cosh \frac{\pi}{h} \right)}{\sinh \frac{\pi}{h}}$$

$$i\bar{\omega} F \rightarrow \frac{\pi^2}{6h^2} C(\bar{\omega})$$

$$C(\bar{\omega}) \rightarrow 1 + i\bar{\omega} \left(\gamma + \log_e \frac{\bar{\omega}}{2} + \frac{i\pi}{2} \right)$$

$$\frac{C}{D} \rightarrow \left(1 + \frac{\pi^2}{6h^2} \right) \left\{ 1 - i\bar{\omega} \left(1 + \frac{\pi^2}{6h^2} \right) \bar{E} \right\}.$$

The use of these limiting forms enables the hinge-moment derivatives to be estimated for $\omega = 0$.

4. *Application of Method.*—In order to apply the method developed in this paper to a particular aerofoil-control combination it is necessary to find appropriate values of the steady-motion derivatives a_2, m_2 and b_2 . In the two applications given below it was not possible to measure these derivatives on the same model as that used for the unsteady tests, although this will be done at a later date. The required values were therefore obtained from other tests; it is thought unlikely that any errors thus introduced would make a significant difference to the estimated oscillatory derivatives.

(a) *Aileron* ($E = 0.2$).—To enable comparison with Wight's results, referred to in section 1, values of the steady derivatives were required for the NPL 282 aerofoil section with a 20 per cent control. The derivative b_2 was obtained directly from Wight's tests, but unfortunately values of a_2 and m_2 could not be obtained from this source without considerable modification of the apparatus. However, the results of tests made by Bryant, Halliday and Batson⁶ (1950) on a similar aerofoil-control combination are available, and from these values of a_2, b_2 and m_2 were obtained. The derivatives a_2 and b_2 were measured in the N.P.L. 7-ft Wind Tunnels Nos. 2 and 3, m_2 being measured in the latter tunnel only. It was found that the mean value of b_2 obtained from these tests agreed closely with Wight's result and so the mean value of a_2

was also assumed to be appropriate. These values, together with the single value of m_2 , were used to determine the equivalent profile (section 2(a), equation (5)). For a Reynolds number of about 10^6 and with transition fixed at $0.1c$, the values of the steady motion derivatives taken were :

$$a_2 = 2.117, \quad b_2 = -0.445, \quad m_2 = -0.404 \text{ (quarter-chord axis).}$$

The equivalent thin profile calculated from equation (5) for a control incidence of 5 deg is shown in Fig. 2.

In Figs. 4 and 5 the estimated hinge-moment derivatives are shown plotted against the reduced frequency parameter, ω . The experimental results given are for a Reynolds number of 0.94×10^6 with transition fixed at $0.1c$ from the leading edge. Estimated values for both free-stream and wind-tunnel conditions are given. Tunnel-wall interference effects appear to be negligible for ω greater than 1.5, and are not large for lower values except when $\omega \rightarrow 0$.

(b) *Tab* ($E = 0.04$).—The oscillatory hinge-moment derivatives for a 4 per cent control on the NPL 282 section have recently been measured by Wight and a comparison with estimated values is given here. Considerable difficulty was experienced in obtaining appropriate values of a steady-flow characteristics of the aerofoil-tab combination. The values of a_2 used were derived from the charts given in Ref. 6, and are in fair agreement with a measured value for a 4 per cent tab on a 1541 (NPL 282) section with a 19 deg (15 deg on basic 1541) trailing-edge angle. No measurements of m_2 for the 1541 section with a 4 per cent tab have been made and the values taken were obtained from a_2 and an estimation of the aerodynamic centre of the system⁷ The derivative b_2 was obtained directly from Wight's tests. The actual values taken were

Transition at	0.1c	0.4c
$a_2 =$	0.64	0.72
$m_2(\frac{1}{4}) =$	-0.174	-0.196
$b_2 =$	-0.280	-0.366

The equivalent thin profile, for a tab deflection of $\gamma = 5$ deg, is shown in Fig. 3.

In Figs. 6 and 7 estimated and measured values of the tab hinge-moment stiffness (t_γ) and damping (t_δ) derivatives are shown plotted against frequency parameter. Results for two transition positions are shown, these being $0.1c$ and $0.4c$ from the leading edge of the aerofoil. Although the steady experimental data used was obtained at a Reynolds number of about 10^6 , measured values of the unsteady derivatives are given for Reynolds numbers of 1, 2, and 3×10^6 . The values for the lowest Reynolds number are least accurate because of the very small forces involved and it is thought to be of value to compare the higher Reynolds number measurements with the estimated values. Good agreement is obtained, particularly for the higher Reynolds numbers. Part of the discrepancy between the theoretical and experimental values of the damping derivative at low values of the frequency parameter, ω , may be due to tunnel interference, since the free-stream theoretical values tend to infinity as $\omega \rightarrow 0$, whereas the experimental values, uncorrected for tunnel interference, remain finite as $\omega \rightarrow 0$. The estimated limiting value of the damping derivative, with an allowance for tunnel-wall interference effects included is shown on Fig. 7.

5. *Concluding Remarks*.—The theory developed in this report appears to be adequate for the type of problem considered, although some doubt must arise from the inconsistency of the steady-motion results used in the example calculated. It is hoped that a proper estimation of the accuracy of the method can be obtained when the steady-motion derivatives a_2 and m_2 are measured by Wight.

List of Symbols

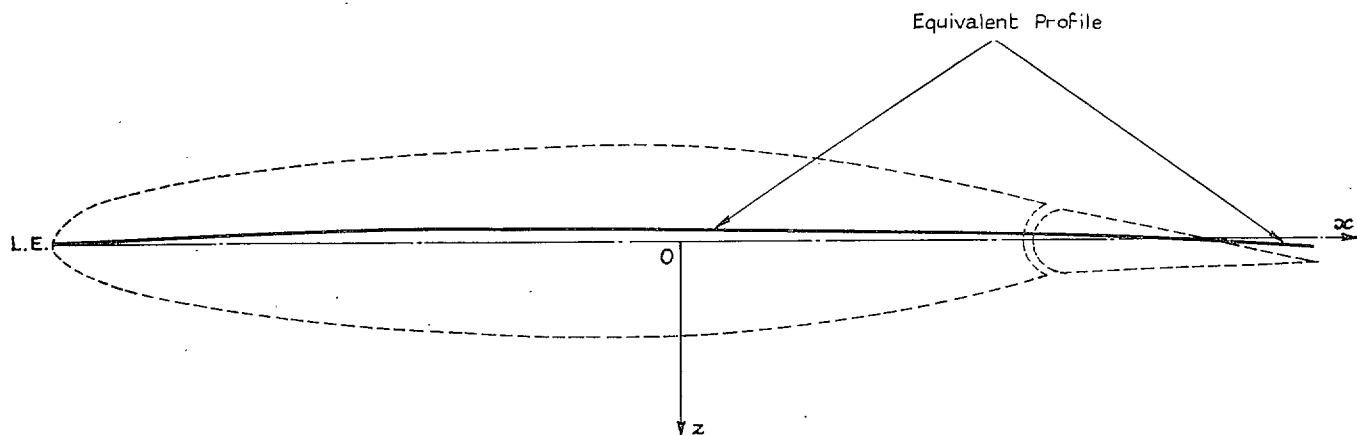
\dot{p}	Frequency of oscillation in radians/second
c	Aerofoil chord
Ec	Control chord
V	Stream velocity at infinity
ρ	Air density
$\omega \left(\equiv 2\bar{\omega} \equiv \frac{\dot{p}c}{V} \right)$	Reduced frequency parameter
η	Mean control incidence
β_0	Amplitude of oscillation
$\frac{1}{2}hc$	Tunnel height
$\gamma = \frac{\bar{\omega}h}{\pi}$	
$L (\equiv \frac{1}{2}\rho V^2 c C_L)$	Total lift
$M(x_0) (\equiv \frac{1}{2}\rho V^2 c^2 C_M(x_0))$	Pitching moment about x_0
$H (\equiv \frac{1}{2}\rho V^2 E^2 c^2 C_H)$	Hinge moment
$a_2 = \frac{\partial C_L}{\partial \beta}, \quad b_2 = \frac{\partial C_H}{\partial \beta}, \quad m_2 = \frac{\partial C_M}{\partial \beta}$	
$\bar{\Gamma}_0 = 2 \cot \frac{\theta}{2}$	
$\bar{\Gamma}_1 = -2 \sin \theta + \cot \frac{\theta}{2}$	
$\bar{\Gamma}_n = -2 \sin n\theta, \dots n \geq 2$	
$\Gamma_0 = 2C(\bar{\omega}) \cot \frac{\theta}{2} + 2i\bar{\omega} \sin \theta$	
$\Gamma_1 = -2 \sin \theta + \cot \frac{\theta}{2} + i\bar{\omega} \left(\sin \theta + \frac{\sin 2\theta}{2} \right)$	
$\Gamma_n = -2 \sin n\theta + i\bar{\omega} \left(\frac{\sin (n+1)\theta}{n+1} - \frac{\sin (n-1)\theta}{n-1} \right), \dots n \geq 2$	
$C(\bar{\omega})$	Theodorsen's lift function, tabulated in Ref. 2
$F = \frac{\pi^2}{6h^2} X_0 e^{-i\bar{\omega}} \left(1 - \frac{i}{\bar{\omega}} \right) - i\bar{\omega} X_0 (P - Q)$	
$X_0 = C(\bar{\omega}) J_0(\bar{\omega}) + i(1 - C(\bar{\omega})) J_1(\bar{\omega})$	
$P = \int_{\bar{\omega}}^{\infty} \frac{e^{-iy}}{y} dy$	
$Q = 2e^{-i\bar{\omega}} \sum_0^{\infty} \frac{e^{-(2n+1)\pi/h}}{2n+1+i\gamma}$	
J_n	Bessel function of n^{th} order.

REFERENCES

<i>No.</i>	<i>Author</i>	<i>Title, etc.</i>
1	W. P. Jones	Aerofoil oscillations at high mean incidences. R. & M. 2654. April, 1948.
2	I. T. Minhinnick	Tables of functions for evaluation of wing and control surface flutter derivatives for incompressible flow. R.A.E. Report Structures 86. A.R.C. 13,730. July, 1950.
3	K. C. Wight	Measurements of two-dimensional derivatives on a wing-aileron-tab system with a 1541 section aerofoil. Part I. Direct aileron derivatives. A.R.C. 15,292. October, 1952.
4	W. P. Jones	Aerodynamic forces on wings in simple harmonic motion. R. & M. 2026. February, 1945.
5	W. P. Jones	Wind tunnel interference effects on measurements of aerodynamic coefficients for oscillating aerofoils. R. & M. 2786. September, 1950.
6	L. W. Bryant, A. S. Halliday and A. S. Batson.	Two-dimensional control characteristics. R. & M. 2730. March, 1950.
7	L. W. Bryant and H. C. Garner ..	Control testing in wind tunnels. R. & M. 2881. October, 1950.

APPENDIX

$$\begin{aligned}
 I_1 &= \int_{\theta_H}^{\pi} \cot \frac{\theta}{2} (\cos \theta - \cos \theta_H) \sin \theta \, d\theta \\
 &= \pi \left(\frac{1}{2} - \cos \theta_H \right) - \left\{ \frac{\theta_H}{2} - \theta_H \cos \theta_H + \sin \theta_H - \frac{\sin 2\theta_H}{4} \right\} \\
 I_2 &= \int_{\theta_H}^{\pi} \sin \theta (\cos \theta - \cos \theta_H) \sin \theta \, d\theta \\
 &= -\frac{\pi}{2} \cos \theta_H + \left\{ \frac{\theta_H \cos \theta_H}{2} - \frac{\sin \theta_H}{4} - \frac{\sin 2\theta_H \cos \theta_H}{4} + \frac{\sin 3\theta_H}{12} \right\} \\
 I_3 &= \int_{\theta_H}^{\pi} \sin 2\theta (\cos \theta - \cos \theta_H) \sin \theta \, d\theta \\
 &= \frac{\pi}{4} - \left\{ \frac{\theta_H}{4} - \frac{\sin 2\theta_H}{4} + \frac{\sin 3\theta_H \cos \theta_H}{6} - \frac{\sin 4\theta_H}{16} \right\} \\
 I_4 &= \int_{\theta_H}^{\pi} \sin 3\theta (\cos \theta - \cos \theta_H) \sin \theta \, d\theta \\
 &= -\frac{1}{4} \left\{ \sin \theta_H - \sin 2\theta_H \cos \theta_H + \frac{\sin 4\theta_H \cos \theta_H}{2} - \frac{\sin 5\theta_H}{5} \right\} \\
 I_5 &= \int_{\theta_H}^{\pi} \sin 4\theta (\cos \theta - \cos \theta_H) \sin \theta \, d\theta \\
 &= -\frac{1}{4} \left\{ \frac{\sin 2\theta_H}{2} - \frac{2}{3} \sin 3\theta_H \cos \theta_H + \frac{2}{5} \sin 5\theta_H \cos \theta_H - \frac{\sin 6\theta_H}{6} \right\}.
 \end{aligned}$$



$$\frac{2z}{c} = \beta \{-0.208 + 0.103 \xi + 0.280 \xi^2 - 0.031 \xi^3\}$$

FIG. 2. Equivalent profile for NPL 282 Aerofoil section with 20 per cent control deflected 5 deg.

$$\frac{2z}{c} = \gamma \{0.131 - 0.190 \xi - 0.076 \xi^2 + 0.246 \xi^3\} \text{ for transition at } 0.1c. \quad \xi = \frac{2x}{c}$$

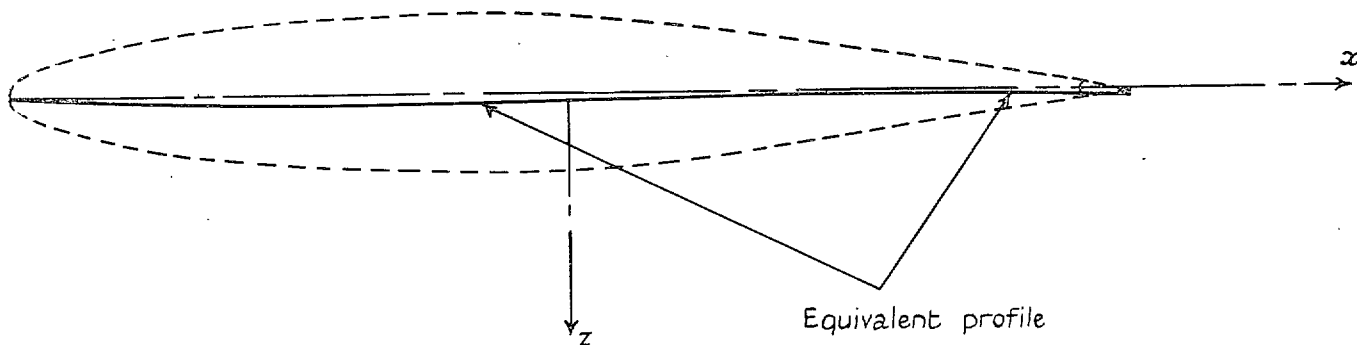


FIG. 3. Equivalent profile for NPL 282 aerofoil section with a 4 per cent tab deflected 5 deg.

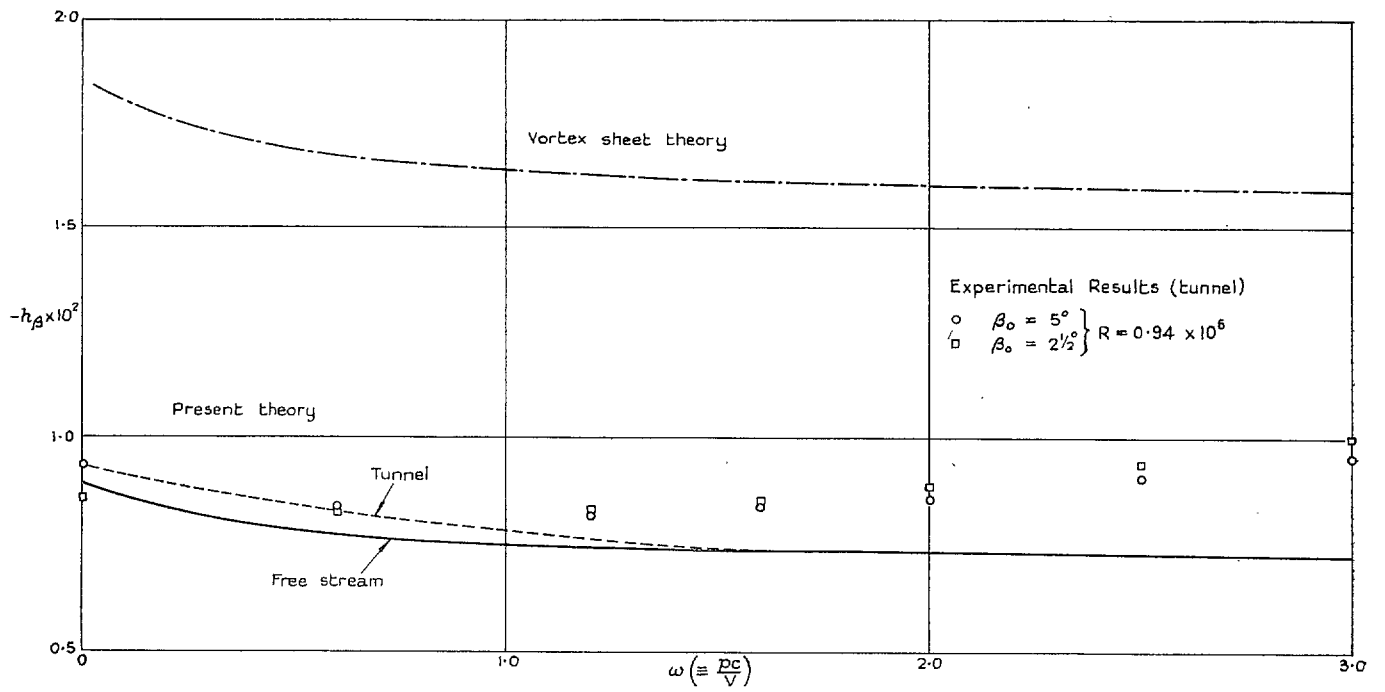


FIG. 4. Hinge-moment stiffness derivative for NPL 282 aerofoil section with a 20 per cent control.

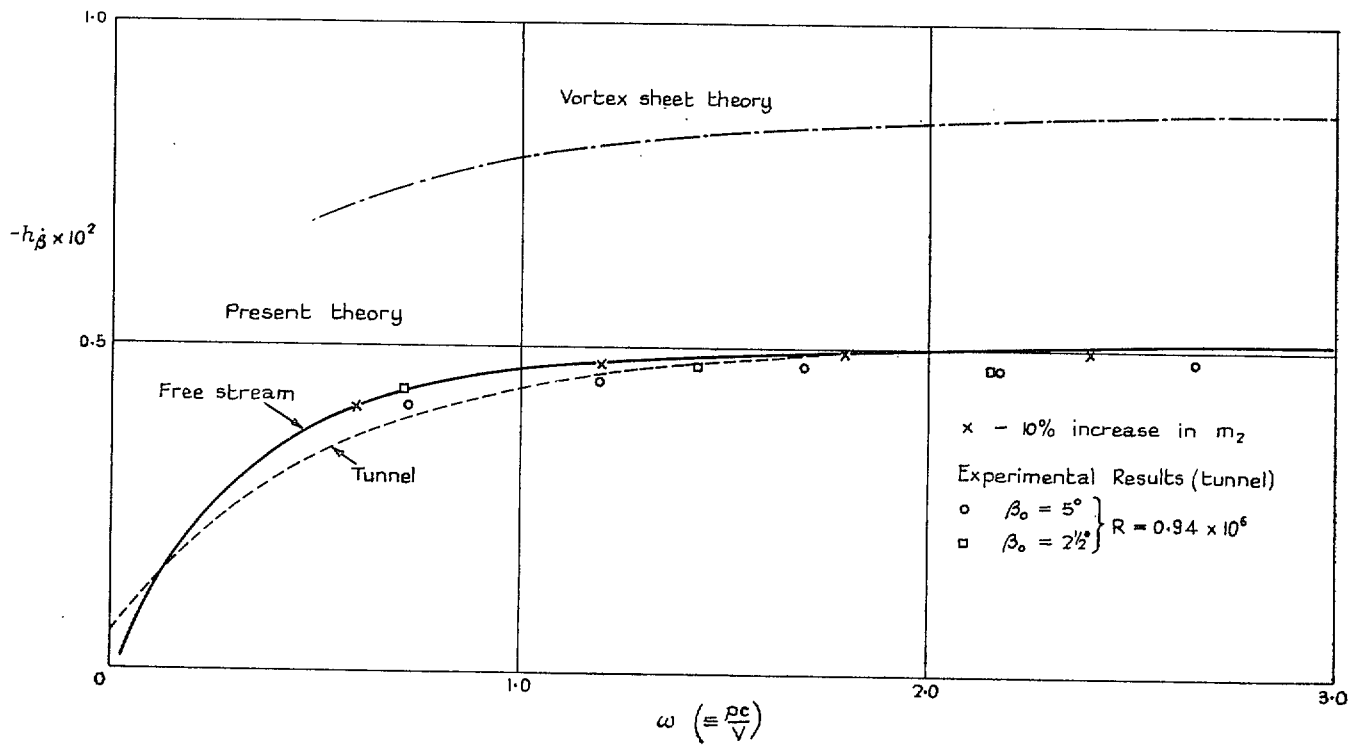


FIG. 5. Hinge-moment damping derivative for NPL 282 aerofoil section with a 20 per cent control.

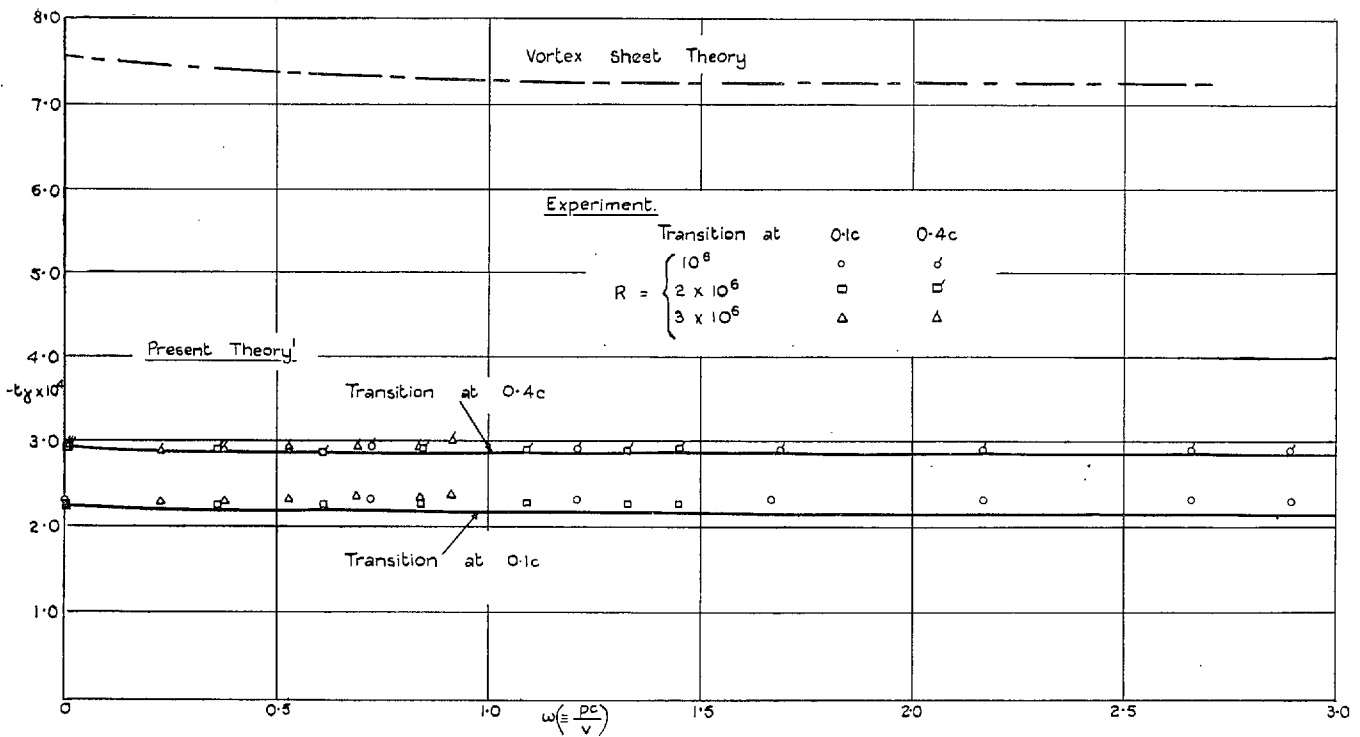


FIG. 6. Hinge-moment stiffness derivative for NPL 282 aerofoil section with a 4 per cent tab.

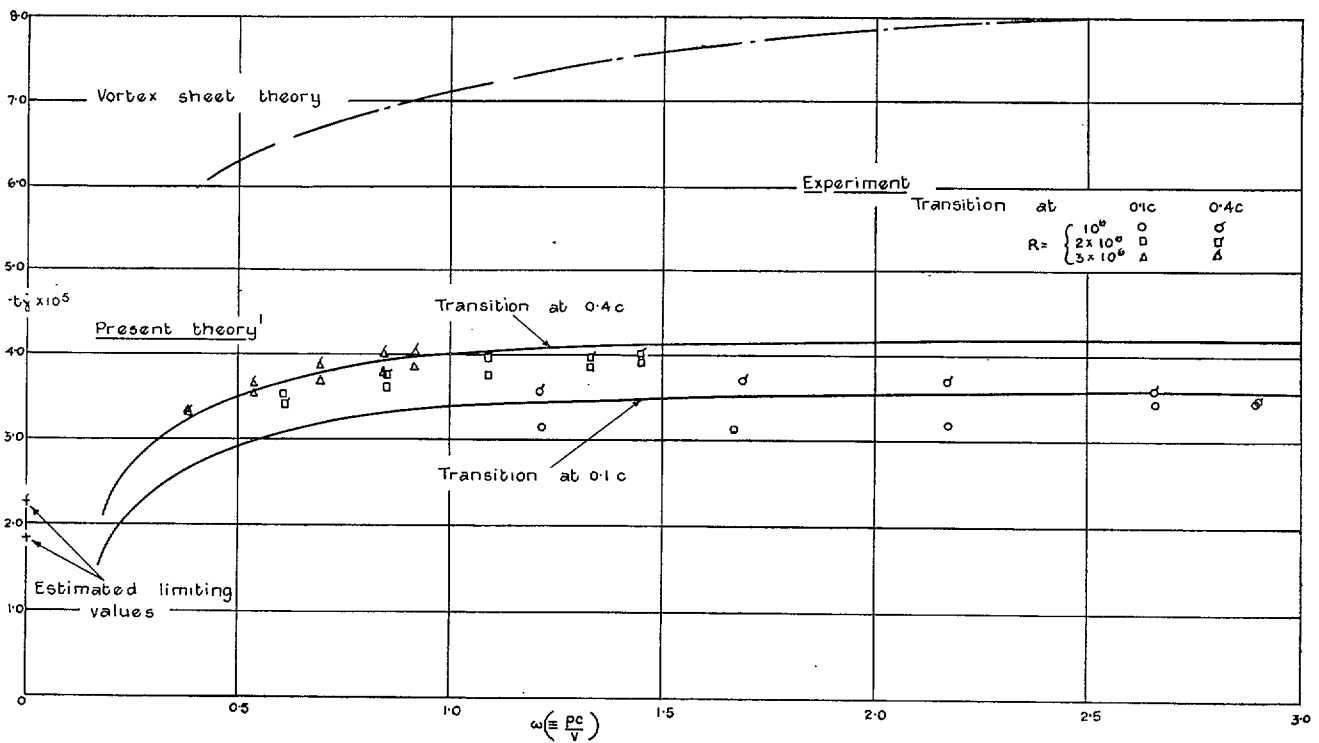


FIG. 7. Hinge-moment damping derivative for NPL 282 aerofoil section with a 4 per cent tab.

Publications of the Aeronautical Research Council

ANNUAL TECHNICAL REPORTS OF THE AERONAUTICAL RESEARCH COUNCIL (BOUND VOLUMES)

- 1938 Vol. I. Aerodynamics General, Performance, Airscrews. 50s. (51s. 2d.)
Vol. II. Stability and Control, Flutter, Structures, Seaplanes, Wind Tunnels, Materials. 30s. (31s. 2d.)
- 1939 Vol. I. Aerodynamics General, Performance, Airscrews, Engines. 50s. (51s. 2d.)
Vol. II. Stability and Control, Flutter and Vibration, Instruments, Structures, Seaplanes, etc. 63s. (64s. 2d.)
- 1940 Aero and Hydrodynamics, Aerofoils, Airscrews, Engines, Flutter, Icing, Stability and Control, Structures, and a miscellaneous section. 50s. (51s. 2d.)
- 1941 Aero and Hydrodynamics, Aerofoils, Airscrews, Engines, Flutter, Stability and Control, Structures. 63s. (64s. 2d.)
- 1942 Vol. I. Aero and Hydrodynamics, Aerofoils, Airscrews, Engines. 75s. (76s. 3d.)
Vol. II. Noise, Parachutes, Stability and Control; Structures, Vibration, Wind Tunnels. 47s. 6d. (48s. 8d.)
- 1943 Vol. I. Aerodynamics, Aerofoils, Airscrews. 80s. (81s. 4d.)
Vol. II. Engines, Flutter, Materials, Parachutes, Performance, Stability and Control, Structures. 90s. (91s. 6d.)
- 1944 Vol. I. Aero and Hydrodynamics, Aerofoils, Aircraft, Airscrews, Controls. 84s. (85s. 8d.)
Vol. II. Flutter and Vibration, Materials, Miscellaneous, Navigation, Parachutes, Performance, Plates and Panels, Stability, Structures, Test Equipment, Wind Tunnels. 84s. (85s. 8d.)

ANNUAL REPORTS OF THE AERONAUTICAL RESEARCH COUNCIL—

1933-34	1s. 6d. (1s. 8d.)	1937	2s. (2s. 2d.)
1934-35	1s. 6d. (1s. 8d.)	1938	1s. 6d. (1s. 8d.)
April 1, 1935 to Dec. 31, 1936	4s. (4s. 4d.)	1939-48	3s. (3s. 2d.)

INDEX TO ALL REPORTS AND MEMORANDA PUBLISHED IN THE ANNUAL TECHNICAL REPORTS, AND SEPARATELY—

April, 1950 - - - - - R. & M. No. 2600. 2s. 6d. (2s. 7½d.)

AUTHOR INDEX TO ALL REPORTS AND MEMORANDA OF THE AERONAUTICAL RESEARCH COUNCIL—

1909-January, 1954 - - - - - R. & M. No. 2570. 15s. (15s. 4d.)

INDEXES TO THE TECHNICAL REPORTS OF THE AERONAUTICAL RESEARCH COUNCIL—

December 1, 1936 — June 30, 1939.	R. & M. No. 1850.	1s. 3d. (1s. 4½d.)
July 1, 1939 — June 30, 1945. -	R. & M. No. 1950.	1s. (1s. 1½d.)
July 1, 1945 — June 30, 1946. -	R. & M. No. 2050.	1s. (1s. 1½d.)
July 1, 1946 — December 31, 1946.	R. & M. No. 2150.	1s. 3d. (1s. 4½d.)
January 1, 1947 — June 30, 1947. -	R. & M. No. 2250.	1s. 3d. (1s. 4½d.)

PUBLISHED REPORTS AND MEMORANDA OF THE AERONAUTICAL RESEARCH COUNCIL—

Between Nos. 2251-2349. - -	R. & M. No. 2350.	1s. 9d. (1s. 10½d.)
Between Nos. 2351-2449. - -	R. & M. No. 2450.	2s. (2s. 1½d.)
Between Nos. 2451-2549. - -	R. & M. No. 2550.	2s. 6d. (2s. 7½d.)
Between Nos. 2551-2649. - -	R. & M. No. 2650.	2s. 6d. (2s. 7½d.)

Prices in brackets include postage

HER MAJESTY'S STATIONERY OFFICE

York House, Kingsway, London W.C.2; 423 Oxford Street, London W.1 (Post Orders: P.O. Box 569, London S.E.1);
13a Castle Street, Edinburgh 2; 39 King Street, Manchester 2; 2 Edmund Street, Birmingham 3; 109 St. Mary Street,
Cardiff; Tower Lane, Bristol 1; 80 Chichester Street, Belfast, or through any bookseller

S.O. Code No. 23-2923

R. & M. No. 2923